

Cluster Formation and Percolation in Ethanol-Water mixtures

Orsolya Gereben, László Pusztai^{a)}

*Institute for Solid State Physics and Optics, Wigner Research Centre for Physics,
Hungarian Academy of Sciences (Wigner RCP HAS), Konkoly Thege út 29-33, H-1121
Budapest, Hungary*

Systematic molecular dynamics studies, using three different water models and the OPLS-AA ethanol force field, of ethanol-water mixtures over the entire concentration range were reported in an earlier work, and the combinations that provided the best agreement with experimental X-ray diffraction data were selected for each mixture. These simulated systems are further analyzed in this work to examine cluster formation and percolation, using four different hydrogen bond definitions. Percolation analysis revealed that each mixture (even the one containing 80 mol % ethanol) is above the 3D percolation threshold, with fractal dimensions, d_f , between 2.6 to 2.9, depending on concentration. Monotype water cluster formation was also studied in the mixtures: 3D water percolation can be found in systems with ≤ 40 mol % ethanol, with fractal dimensions between 2.53 and 2.84.

Keywords: alcohol-water mixtures; molecular dynamics; hydrogen bonding; cluster formation; percolation

^{a)} Corresponding author: L. Pusztai, Wigner RCP, HAS, H-1525 Budapest, Konkoly Thege út 29-33, Hungary; Tel/fax: + 36 1 392 2589; email: pusztai.laszlo@wigner.mta.hu

1 INTRODUCTION

The structure of alcohol-water solutions has been studied widely by both experimental [1,2,3,4,5] and theoretical [6,7,8] methods, and provided somewhat confusing and contradictory picture. Detailed discussions concerning these preliminaries are provided in the introductory parts of our very recent publications [9,10,11], so these are not repeated here. In these recent works, H-bond connectivities [9], ring formation and statistics [10], and the ‘lacunarity’ [11] have been analyzed. To complete our extensive investigations on water-ethanol mixtures, here characteristics of cluster formation and percolation observable in these systems are presented. To the best of our knowledge, such properties have not been considered before for aqueous ethanol solutions.

Similarly to the aforementioned recent studies of the hydrogen bonded network in water-ethanol mixtures [9,10,11], the basis of the present analyses is our preceding extensive molecular dynamics (MD) investigation [12]. There, a series of MD simulations for ethanol-water mixtures with 20 to 80 mol % ethanol contents, for pure ethanol and water was performed with one ethanol and three different water force fields. The primary aim of that work was to find the potential models that provide the best agreement with experimental X-ray diffraction data. In each mixture the OPLS-AA [13] potential was used for ethanol, in combination with three different water force fields, the rigid SPC/E [14] and TIP4P-2005 [15], as well the rigid polarizable SWM4-DP [16] ones. No single water force field could be identified that would provide the best agreement with experimental data at each concentration: for higher ethanol contents the SWM-DP, whereas at lower ethanol concentrations the TIP4P-2005 potential provided the closest match.

In this work, detailed analyses of the hydrogen-bonded network are provided for the most successful simulations at each concentration, in terms of hydrogen bonded assemblies (clusters) of molecules. The number and size of the clusters strongly depends on the number of hydrogen bonds (HB) which, in turn, is determined by some (somewhat arbitrary) definitions of hydrogen bonds. As discussed (for instance) in our previous paper [9], there is not an exact rule for the definition, but several different approaches can be found in the literature. We have opted for purely geometric definitions: the O---H and O---O distances should fall into a certain distance range, and sometimes there is an additional constraint on the O-H...O angle, as well. A collection of such definitions are introduced and analyzed in Ref. [9]; concerning earlier studies on ethanol-water mixtures, Noskov [17] applied an O---H cutoff of 2.4 Å and O-H...O angle > 150° for defining H-bonds. Our criteria are comparable to these choices (see Ref. [9]). In our previous MD simulation investigation [12] the LOOSE condition for hydrogen bonding was based solely on distance ranges. The upper limiting values were defined by the first minima of the O-O, and by the second (i.e., first intermolecular) minima of the O-H PRDFs. On average, the “H-bonding” ranges were set to be between 2.4 and 3.6 Å for O-O and 1.4–2.7 Å for O-H pairs (see the Supporting Information Tables 1 and 2 in our previous work for details [12]). A STRICT condition with the distance ranges of the LOOSE condition and with an additional angular restriction of O-H...O > 120° was also applied; the 120° value was based on the definition of Chen et al. [18] and on our other previous work [19]. In this paper, similarly to the immediate predecessor [9], four different H-bond definitions were applied, in order to explore how cluster formation might depend on the choice of the cutoff conditions. Apart from the LOOSE (L), and STRICT120 (S120) conditions (STRICT120 being the same as

the STRICT in the previous paper [12]), STRICT140 (S140) with $\text{O-H}\dots\text{O}>140^\circ$ and STRICT150 (S150) with $\text{O-H}\dots\text{O}>150^\circ$ are also applied for each simulation result.

Percolation theory is frequently and successfully applied for explaining some of the unusual macroscopic features of hydrogen-bonded systems like water [20,21,22,23] and aqueous solutions [24]. Liquid water can be described by bond-percolation theory as a gel-like network with bent (and to some extent, broken) hydrogen bonds, well above the percolation threshold [20]. Dividing oxygen atoms into categories based on the number of their intact hydrogen bonds can be considered as a polychromatic correlated site percolation problem. The infinite hydrogen-bonded network in simulated water was found to contain patches of four-bonded water molecules with structures less ramified than that could be expected from their random distribution. This way, the anomalous behavior of, for example, the isothermal compressibility, constant-pressure and constant-volume specific heat and thermal expansion could be predicted and to some extent, explained [21]. The local density in the vicinity of these spatially correlated four-bonded patches was found to be lower than the global density [22]. According to random site percolation theory, the infinite open clusters are true fractals at the percolation threshold with fractal dimensions $f_d=2.53$ for the 3D, and $f_d\approx 1.896$ for the 2D case [25]. Based on the fractal dimension, a different percolation behavior was detected in tetrahydrofuran-water mixtures by Oleinikova et al. [24]. The predicted immiscibility gap was in good agreement with the concentration interval where both water and the solute were above their respective 3D percolation threshold. This suggested that totally miscible solutions can only exist if not both of the two compounds percolate in 3D [24]. Here, we wished to establish the

percolation behavior of ethanol-water mixtures, so that later similar analyses may be conducted.

The paper is organized in the following way: Section 2 briefly describes the computational methods used, while in Section 3, results on the cluster distributions and percolation properties are given in detail. Finally, Section 4 summarizes our findings.

2 METHODS

2.1 Molecular dynamics simulations

Details of the MD simulations are given in our previous paper [12] and therefore here only a brief description is appropriate. All MD simulations were performed by the GROMACS 4.0 simulation package [26], in the NVT ensemble at $T=293$ K. The simulation length was 2000 ps in each case. Particle configurations in the production phase were collected 20 ps apart and in the end, 76 configurations were used for calculating average cluster sizes, connectivities and morphologies.

Calculations reported here are identified by their ethanol content and by the first letter of the water force field applied (see Table 1); for example, ‘Et60S’ refers to the mixture containing 60 mol % ethanol where the MD simulation was performed by using the SWM4-DP water force field (Table 1).

Table 1. Simulation names and densities for the MD simulations.

c_E (%) ^a	Simulation name	n_E ^b	n_W ^c	ρ_E (Å ⁻³) ^d	ρ_W (Å ⁻³) ^e	ρ (Å ⁻³) ^f	ρ_{liq} (g/cm ³) ^g
100	Et100	1331	0	0.0103	0.0000	0.0930	0.790
80	Et80S	1226	316	0.0096	0.0025	0.0940	0.799
60	Et60S, Et60T	1093	715	0.0088	0.0057	0.0960	0.816
40	Et40T	889	1328	0.0073	0.0109	0.0985	0.837
20	Et20T	571	2280	0.0047	0.0188	0.0990	0.841
0	Et0S, Et0T	0	3993	0.0000	0.0330	0.0990	0.987

^aethanol concentration in mol %.

^bnumber of ethanol molecules.

^cnumber of water molecules.

^dmolecular number densities of ethanol molecules.

^emolecular number densities of water molecules.

^fatomic number density of all the atoms in the simulation cell.

^gdensity of the liquids.

2.2 Cluster analyses

Analyses of the hydrogen-bonded clusters/network was performed by our own C++ computer code, specifically developed for this purpose, using a depth-first search algorithm for identifying clusters (see also Refs. [9,10,11]). The term ‘cluster’ is applied only for molecules connected by hydrogen bonds (i.e., lone molecules are not considered as clusters). Sometimes the distinction is made between cluster (no percolation) and network (percolation is present), but generally the term ‘cluster’ is used to describe assemblies of hydrogen bonded molecules, regardless their percolation properties. During the HB determination the system was treated as an isolated system, as in the work of Geiger et al. [20], namely that only one instant of the periodic box – and consequently, each hydrogen

bond – was used, even though hydrogen bonds were determined using the minimum image convention.

Cycle perception was performed by the same software; detailed results can be found in Ref. [10].

2.3 Percolation

Percolation properties of each system were also analyzed by the computer code mentioned above. For each cluster of each configuration of every system, it was determined whether the cluster in question was infinite; if it was then in how many dimensions. In general, a cluster is said to percolate if there is an infinite open cluster in at least one dimension. In this work the term ‘network’ is applied to a 3D percolating infinite cluster. Fractal dimensions have been calculated using the box-counting method, by the same software.

3 RESULTS AND DISCUSSION

Having determined the H-bonds, clusters (molecules connected by HB-s) were identified; some of their statistical descriptors, as a function of the actual H-bond definition, have already been discussed in detail in Ref. [9].

3.1 Number of clusters

The average number of clusters for all the systems were calculated, and are shown in Fig. 1. Results for cluster sizes and distributions for the less strict HB conditions are shown,

as well, in order to see the extent the choice affects the results. For the same simulation with different HB conditions the number of clusters is increasing with the increasing angular cutoff, as expected, similarly to the number of lone molecules. Regarding these values for the same HB condition for different concentrations, the number of clusters is generally increasing monotonically with increasing ethanol concentration, although there is a maximum around the Et40-Et60 region, especially for the stricter HB conditions. Comparing the values of the Et60S and Et60T simulations, there is not much of a difference between the L and S conditions (Et60S is a bit larger). On the other hand, there is a substantial difference between the S140 and S150 conditions, where Et60T shows a higher value. Interestingly, for the pure water models always the value of the Et0T simulation is a bit higher than that for Et0S. It is notable that the number of clusters for pure ethanol is substantially higher than it is for the mixtures, indicating a very different cluster formation, as discussed later.

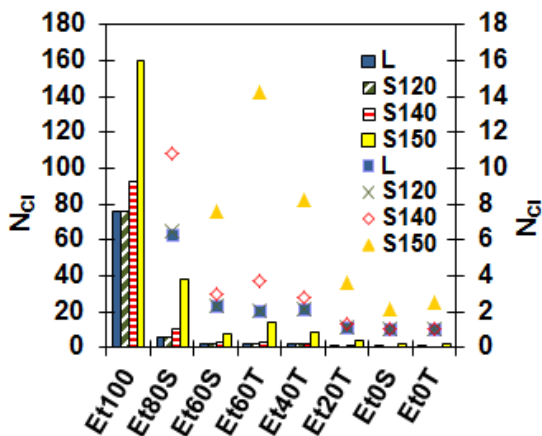


Fig. 1. Average numbers of clusters/configuration for ethanol-water mixtures, for pure ethanol and for pure SWM4-DP (denoted as ‘Et0S’) and TIP4P-2005 (Et0T) water. Values belonging to the columns can be read on the left y-axis, while the smaller cluster numbers

(particularly for water contents above 40 molar %) are represented by markers and can be read on the right (blown-up) y-axis, too, for the sake of clarity.

3.2 *Cluster size distributions, percolation*

Cluster sizes for all the simulations were calculated using all the four HB conditions. The number of clusters versus the total number of molecules in the clusters is shown in Fig. 2(a), the small cluster size range is enlarged in Fig. 2(b), and panel (c) and (d) depict the participation of water and ethanol molecules separately. The values for the L and S120 HB conditions are almost identical, so only case L is shown. Distributions for pure ethanol for the various HB conditions are significantly different from the distributions of the water-containing systems. While for all the systems there are some small size clusters, there are more of them when the HB condition becomes stricter. Their numbers quickly decrease with increasing cluster size; the maximum size of these small clusters is the largest (~200 molecules) for pure ethanol, and decreasing to 1 to 5, depending on the water force field and the HB condition. There is a peak with a characteristic cluster size (the mean cluster size for the peak) for the water-containing systems, see Table 2. The majority of the molecules (86% for S150, 98% for the L condition for Et80S; 96 to ~100% for the other models and conditions) are in this main cluster; there is one main cluster in each configuration of these systems. The width of the peak, as characterized by the standard deviation (also given in Table 2), is not changing much for the L, S120 and S140 HB conditions, although it is increased somewhat for the S150 HB condition. At the same time, the characteristic cluster size decreases a bit. It is also apparent that Et60S have larger characteristic cluster sizes than Et60T for the stricter conditions, while for pure water the

characteristic sizes are the same for the two force fields for all conditions (SWM4-DP showing a slightly larger width though).

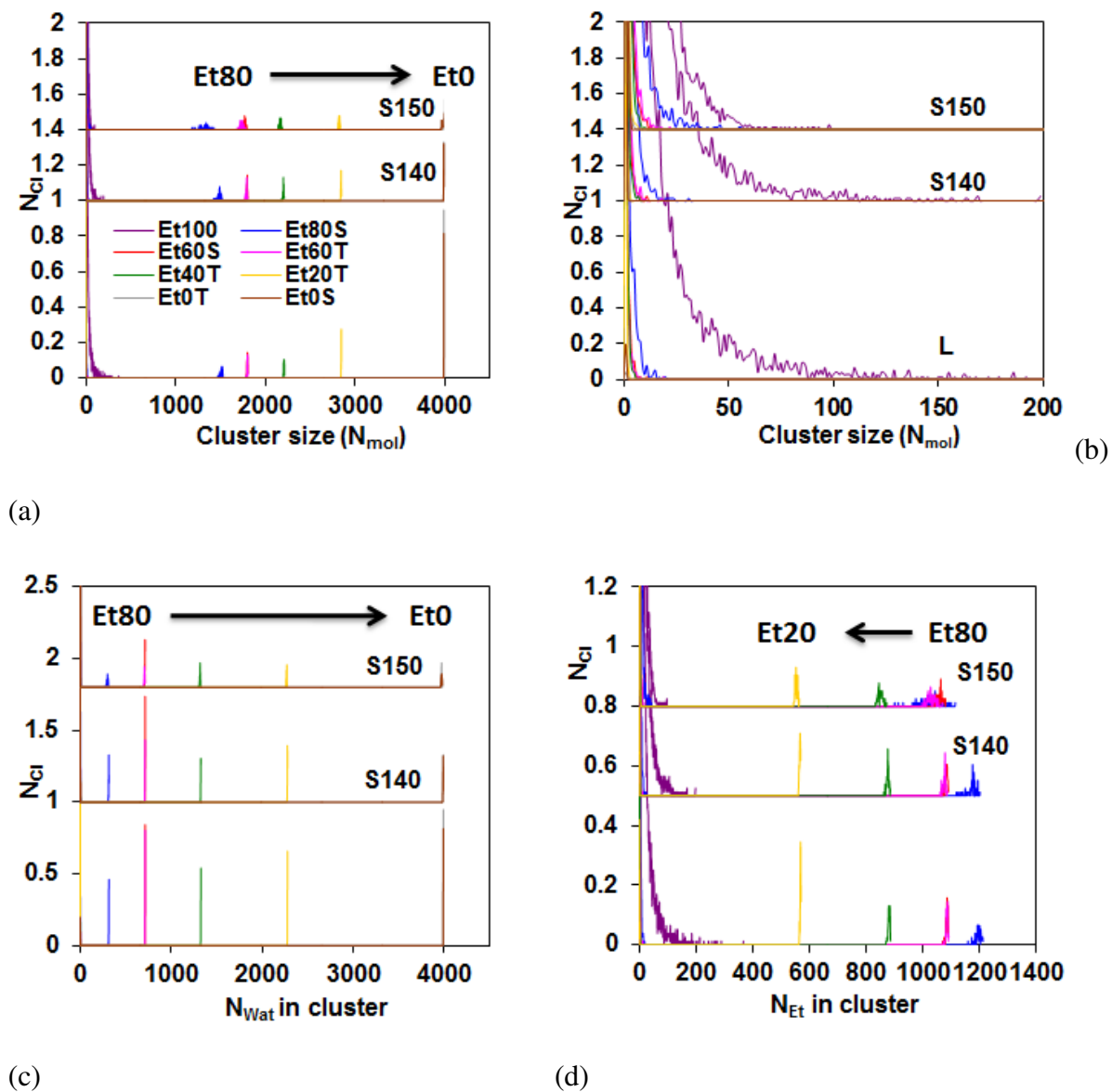


Fig. 2 (a) Cluster size (the total number of molecules in the cluster) distributions for all the simulations; (b) the same as (a), with an enlarged small cluster size region; (c) the number of clusters versus the number of water molecules in the clusters; (d) the number of clusters

versus the number of ethanol molecules in the cluster. The legend is only given in panel (a), it is the same for the other panels as well.

Table 2. Characteristic cluster sizes (with standard deviations) for the percolating main clusters in the water-containing simulation boxes. Values in brackets are the percentages of the molecules that participate in the main cluster, as related to the total number of molecules or to the total number of ethanol molecules respectively.

Name	$N_{\text{tot}}^{\text{a}}$				N_{Et}^{b}			
	L	S120	S140	S150	L	S120	S140	S150
Et80S	1513±11 (98.1)	1512±12 (98.1)	1487±19 (96.5)	1329±46 (86.2)	1198±10 (97.7)	1197±11 (97.7)	1174±17 (95.6)	1030±40 (84.0)
Et60S	1801±4 (99.6)	1801±4 (99.6)	1798±6 (99.4)	1775±11 (98.2)	1087±4 (99.4)	1087±4 (99.4)	1083±6 (99.1)	1062±10 (97.1)
Et60T	1801±4 (99.6)	1801±4 (99.6)	1792±7 (99.1)	1738±16 (96.1)	1087±4 (99.4)	1086±3 (99.4)	1078±6 (98.6)	1031±14 (94.4)
Et40T	2209±4 (99.6)	2209±4 (99.6)	2204±5 (99.4)	2169±10 (97.9)	882±3 (99.2)	882±3 (99.2)	877±4 (98.7)	851±8 (96.8)
Et20T	2849±2 (99.9)	2849±2 (99.9)	2846±2 (99.8)	2825±6 (99.1)	569±1 (99.7)	569±1 (99.7)	567±2 (99.3)	555±4 (97.2)
Et0S	3993±0.4 (~100)	3993±0.5 (~100)	3991±1 (99.95)	3974±5 (99.5)				
Et0T	3993±0.3 (~100)	3993±0.3 (~100)	3992±1 (99.95)	3974±4 (99.5)				

^atotal number of molecules.

^bnumber of ethanol molecules.

Percolation analysis was performed and revealed the presence of an infinite open cluster, with 3D percolation, in all the water-containing systems. On the other hand, percolation analysis in Et100 (pure ethanol) revealed that only in cases of the (less strict) L, S120 and S140 HB conditions can one single 1D infinite cluster be found, in one configuration of the configuration ensemble. This amounts to an occurrence probability of 1.3%, way below the percolation threshold; note that no percolation at all could be detected if the strictest (S150) HB condition was used. Due to the percolation in the water-containing systems the actual characteristic cluster size would depend on the size of the simulation box, but the percentages of the molecules involved (given in brackets in Table 2) and the trend how it is changing with the concentration and HB condition would remain similar.

Fractal dimensions for the percolating clusters were also calculated and are displayed in Table 3. The values increase from $d_f=2.60$ to 2.99 with increasing water concentration, and all of them are above $d_f=2.53$, which is the 3D percolation threshold predicted by random site percolation theory [25]. If the fractal dimensions are plotted against the ethanol concentration (given in molar %), a nearly linear behavior can be found; only the value for the Et80S simulation at the S150 HB condition is a bit lower, see Fig. 3.

Table 3: Average fractal dimensions with standard deviations for the percolating main clusters of the ethanol-water mixtures and pure water.

Name	L	S120	S140	S150
Et80S	2.67±0.006	2.67±0.006	2.66±0.008	2.60±0.018
Et60S	2.73±0.004	2.73±0.004	2.73±0.004	2.72±0.004
Et60T	2.74±0.003	2.74±0.003	2.73±0.004	2.72±0.006
Et40T	2.81±0.003	2.81±0.003	2.81±0.003	2.80±0.004

Et20T	2.90 ± 0.002	2.90 ± 0.002	2.90 ± 0.002	2.90 ± 0.003
Et0S	2.99 ± 0.001	2.99 ± 0.001	2.99 ± 0.001	2.99 ± 0.001
Et0T	2.99 ± 0.001	2.99 ± 0.001	2.99 ± 0.001	2.99 ± 0.001

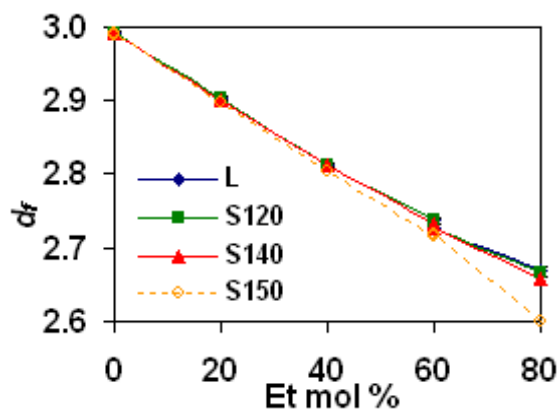


Fig. 3. Fractal dimension versus the ethanol concentration (in molar %) for the percolating systems.

Considering the number of water and ethanol molecules in the clusters (Fig. 2 (c) and (d) and Table 2) three interesting things can be observed:

- 1) While the number of water molecules in the main clusters increases monotonically with decreasing ethanol concentration for all HB conditions (explicit values are not given, only total number of molecules and number of Et), the number of ethanol molecules monotonically decreases with decreasing ethanol concentration for only the L, S120 and S140 HB conditions. The characteristic size for the S150 HB condition in the Et80S simulation is a bit lower than it is for the Et60 simulations.

- 2) There is not much variation in terms of the number of water molecules in the clusters across the individual particle configurations, the number of ethanol molecules shows almost the same standard deviation as the total number of molecules.
- 3) The participation of ethanol molecules in the main cluster is between 84.0 and 99.7% (if we omit the lowest value, which occurs in the Et80S system using the S150 condition, they change between 94.4-99.7%) while for the water molecules it is 94.8 to ~100%.

The occurrence of purely ethanol and purely water clusters among the small (binary) clusters was also determined; the results are shown in Fig. 4, as a percentage of the number of clusters. While for ethanol the percentage increases from ~7% to ~76% with increasing ethanol concentration, it declines quickly for pure water clusters from 14% to 0% with decreasing water concentration. The percentage of molecules compared to the total number of molecules in their own type is small: the largest value is ~7% and quickly declines to 0.02% for ethanol with decreasing ethanol concentration. Large differences between the values corresponding to the different HB conditions were observed, in favor of the strictest S150 condition. The maximum number of molecules in a purely ethanol cluster is 13 to 15 for the Et80S systems, but only 2 to 5 for the most diluted Et20T system. For water the percentage of the water molecules involved in pure water clusters is <0.05%, and most of them consist of two (or at most of three, in rare occasions) molecules. This shows that ethanol has a larger affinity to form small, pure clusters, especially in the high ethanol concentration range, than water. At the same time, at low concentration (~20% ethanol) there is no evidence of substantial chainlike cluster formation, in contradiction to the suggestions of Sato et al. [5].

Based on the cluster analysis we can conclude that the aggregation properties of pure ethanol are different from the rest of the systems: there are many, smaller sized clusters, and virtually no percolation can be found in the system. The water-containing mixtures have aggregation characteristics similar to water, as even the Et80S system is above the 3D percolation threshold. These mixtures contain a binary infinite open cluster (network), and some smaller clusters can be found, as well. It can therefore be established that the percolation threshold for ethanol-water mixtures lies somewhere in the 80 to 100 mol % ethanol region. It is interesting to notice that in the analysis of the excess activation enthalpy and entropy of these systems, by Sato et al. [5], a change of the slope of both of these quantities versus the ethanol concentration can be observed at ~90 mol % ethanol concentration. The excess partial molar enthalpy and entropy for water also changes its slope, and increases in this region. As these quantities are considered to be the consequences of multiple interactions between ethanol and water, it is tempting to suggest that these changes can be related to the percolation threshold of binary clusters in the system. It is also apparent that system Et60S has larger characteristic cluster sizes than system Et60T for the stricter conditions. On the other hand, for pure water the characteristic sizes are the same for the two force fields for all conditions.

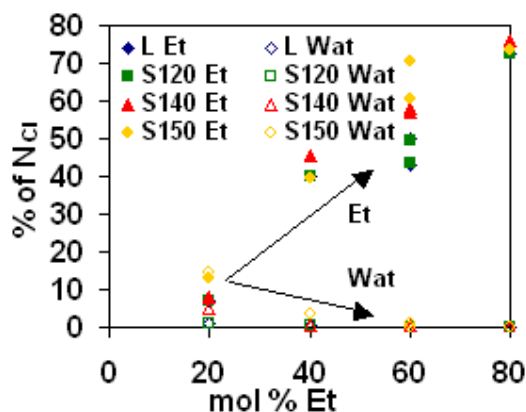


Fig. 4. The percentage of pure ethanol and water clusters among the small clusters.

3.3 *Monotype cluster formation*

So far all types of hydrogen bonds were considered during cluster formation. Now we will only consider hydrogen bonds between the same types of molecules, as this can reveal information about the possible inner structure of the clusters. It has to be noted that these monotype clusters are mostly parts of larger, binary clusters, and only a portion of them are pure isolated clusters. Statistics concerning the pure isolated clusters were given in the previous section.

The cluster/network analysis was performed similarly as for the binary clusters, but first only for the ethanol molecules, and then only for the water molecules in the particle configurations. The analysis was done for all the HB conditions, and gave similar results concerning observable trends. Here the results only for the most reasonable, S150 HB condition will be given. Statistics concerning the monotype clusters are shown in Fig. 5, where the respective concentrations of the investigated molecule types are given; that is, values for monotype ethanol clusters of the 20 mol % ethanol containing simulation are compared to values of monotype water cluster formation found in the simulated system with 80 mol % ethanol (20 mol % water), and so on.

The number of molecules involved in monotype hydrogen bonding is roughly the same for the 20 mol % ethanol and 20 mol % water simulations, although the total number of ethanol molecules in the latter is almost twice as large. This is reflected by the much higher percentage of involvement (~65% for water, and ~25% for ethanol), see Fig. 5(a). For the higher molar fractions the values for water increase more rapidly than for ethanol: the percentage values show a behavior closer to linear for ethanol, while reaching nearly 100% hydrogen bonding at 60 mol % for water. Regarding the average cluster sizes (Fig. 5 (b))

upper panel) the values are increasing near linearly from ~2 to ~8. For water the values for the least concentrated (20 mol % ethanol) system are similar (~3.5) to ethanol at this concentration.

Considering the number of clusters (see Fig. 5(b) lower panel), both ethanol and water have similar values at 20 mol % (~60), but ethanol presents a maximum curve having the largest number of monotype clusters at 80%. On the other hand, the number of water clusters decreases monotonically, except for the value of 40 mol % water when the TIP4P-2005 force field is used. There is a large difference between the values of the TIP4P-2005 and SWM4-DP force field simulations for the 40 mol % water concentration: the SWM4-DP force field brings about higher monotype hydrogen bonding capability, and therefore higher average cluster size and lower number of clusters, in accordance with our previous findings based on the atomic connectivities. Therefore we can conclude that water has higher affinity to form monotype clusters (to have at least one water neighbor), which can be attributed only partially to the larger number of water molecules in the systems.

The low number of clusters suggested that for $\geq 60\%$ water content there might be water percolation in the system, which was confirmed by performing percolation analysis for the monotype water clusters at each concentration. Indeed, three-dimensional percolation was found for $\geq 60\%$ water concentration; the characteristic sizes are shown in Table 4. In case of system Et40T with the S150 HB condition, 95% of the configurations had 3D, while 5% 2D percolation, putting it over the 3D percolation threshold. (The less strict HB conditions had 100% 3D percolation.) The monotype percolating characteristic cluster size is ~45-55% of the respective binary characteristic cluster size shown earlier in Table 2 for the Et40T and ~80% for the Et20T simulations.

Fractal dimensions were calculated for the monotype percolating clusters, as well; they are given in Table 5. The values are between $d_f=2.53$ and 2.6 for the Et40T, and 2.83 and 2.84 for the Et20T simulation, depending on the HB condition. $d_f=2.53$ was found for the Et40T S150 system with 95% 3D percolation, not much above the percolation threshold.

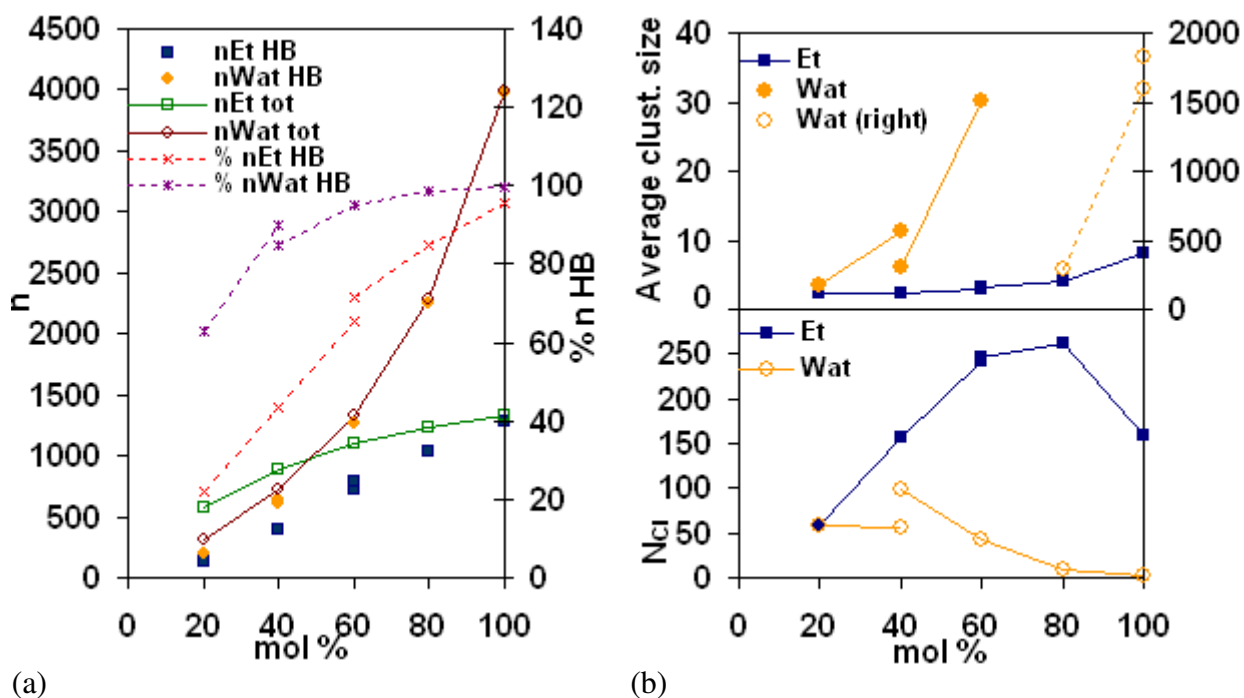


Fig. 5. Statistics concerning the monotype cluster formation for the simulations with different concentrations performed with the S150 HB conditions. (a) Total number of ethanol (nEt tot) and water (nWat tot) (left y-axis), number of ethanol (nEt HB) and number of water molecules (nWat HB) involved in monotype hydrogen bonding (left y-axis), and the percentage of ethanol (% nEt HB) and water (% nWat HB) atoms involved in monotype hydrogen bonding (right y-axis) plotted against the respective molar fractions. b) Upper panel: average monotype cluster sizes and lower panel: number of monotype clusters (N_{Cl}) plotted against the respective molar fractions. The 80 and 100% values for the water clusters are plotted against the right y-axis in the upper panel, and represented by empty

markers for easier distinction. Only data points created by the same force field are connected by a line.

Table 4. Characteristic sizes of the percolating monotype water clusters. Standard deviations are also given. Values in brackets are the percentages of the molecules contained in the monotype percolating cluster compared to the total number of water molecules.

Name	L	S120	S140	S150
Et40T	1223±19 (92.1)	1223±20 (92.1)	1200±28 (90.4)	988±57 (74.4)
Et20T	2271±4 (99.6)	2271±4 (99.6)	2266±5 (99.4)	2235±9 (98.0)
Et0S	3993±0.4 (~100)	3993±0.5 (~100)	3991±1 (99.95)	3974±5 (99.5)
Et0T	3993±0.3 (~100)	3993±0.3 (~100)	3992±1 (99.95)	3974±4 (99.5)

Table 5. Average fractal dimensions for the monotype 3D percolating clusters (both Et60 simulations are mentioned).

Name	L	S120	S140	S150
Et60S	1.73±0.50	1.73±0.50	1.73±0.49	1.71±0.36
Et60T	1.60±0.20	1.60±0.20	1.58±0.27	1.54±0.25
Et40T	2.60±0.01	2.60±0.01	2.59±0.01	2.53±0.07
Et20T	2.84±0.001	2.84±0.001	2.84±0.001	2.83±0.001
Et0S	2.99±0.001	2.99±0.001	2.99±0.001	2.99±0.001
Et0T	2.99±0.001	2.99±0.001	2.99±0.001	2.99±0.001

The difference in the behavior of the 40 mol % water containing simulations, Et60S and Et60T, can be explained by the fact that in Et60T no (monotype) percolation was found in the system. On the other hand, in the case of system Et60S L at the S120 HB condition, two configurations from the examined 76 had one-dimensional and one configuration had two-dimensional percolation. For system S140 at the S150 HB condition one configuration had one dimensional percolation. This shows that the 40 mol % water concentration is somewhat below the percolation threshold, which is defined as the concentration where we can find infinite clusters with 50% probability. The fractal dimension of these systems are all below the 2D percolation threshold of $d_f \approx 1.9$, for Et60T it is between 1.54 and 1.6, and for Et60S it is between 1.71 and 1.74 (see Table 5).

From the behavior of the excess partial molar enthalpy and entropy in the 10-18 mol % ethanol concentration range, calculated from dielectric relaxation measurement data, Sato et al. [5] suggested that the hydrogen bond network of water is disrupted by the ethanol molecules, and ‘percolation nature of water will no longer be present in the region >0.1 Et mol fraction’. Our molecular dynamics results clearly do not support this suggestion, as even in the case of 40 mol % ethanol content 3D water percolation was found, regardless of the water force field and the HB condition. As it was mentioned above, Sato et al. [5] found changes in the slope of the excess activation free energy, enthalpy and entropy around 50 mol % ethanol concentration. They suggested that some structural changes occur in this region. Nishikawa et al. [1] suggested that concentration fluctuations reach their maximum at ~ 40 mol % ethanol, based on small angle X-ray scattering experiments. Ben-Naim [6] found that at ~ 47 mol % ethanol concentration the average affinity between water molecules reaches its maximum, while between ethanol and water molecules, reaches its

minimum. All of these findings can be connected to the fact that, according to our simulation data, the percolation threshold for water can be found somewhere between 40 and 60 mol % ethanol concentration in ethanol-water mixtures. Oleinikova et al. [24] reported the 2D percolation threshold for water in tetrahydrofuran-water mixtures at 53 mol % water concentration, and the 3D threshold at 63 mol % water, which are not far from our results.

At the percolation threshold the mean cluster size distribution follows the critical power law of $n(s) \sim s^{-\tau}$ with $\tau=2.2$. [24,25]. Also characteristic is the appearance of a ‘hump’ at the percolation threshold, connected to the presence of infinite clusters in the system. Usually for concentrations lower than the percolation threshold, positive deviation is found, whereas for higher concentrations negative deviation can be observed. This is clearly visible in Fig. 6 for the Et60T simulations, where no percolation occurred at all, and for the 60 mol % water containing Et40T simulation, which is well above the percolation threshold. The Et60S simulation with the S150 HB condition is still a bit under even the one dimensional threshold (infinite cluster is found with only ~1.3% probability), but in the cluster size of 1 to 9 water molecules region the system exhibits a power law behavior (although the characteristic hump does not appear yet). The Et40T simulation with the L condition is well over the threshold, no real hump can be seen; the dots representing the infinite clusters (one for each configuration) are separated from the other clusters, and can be found around $\log_{10}[s] \sim 3.1$ at the right bottom corner. The curves for the less strict HB conditions (not shown) are very similar. Therefore it can be concluded that the choice of the water force field has a more significant effect on the percolation threshold than the choice of the applied HB condition using the same force field.

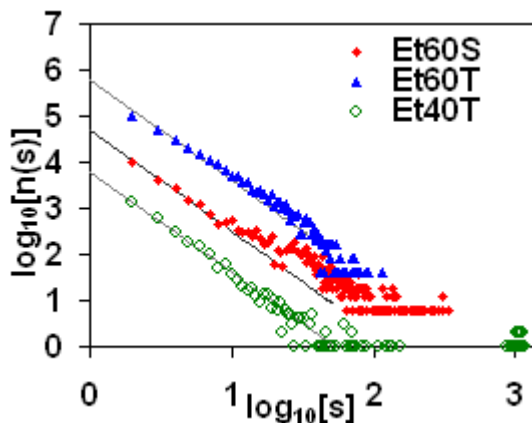


Fig. 6. The logarithm of the mean size distribution to base ten of the monotype water clusters plotted against the logarithm of the sizes to base ten for the Et60S, Et60T and Et40T simulation results with the S150 HB condition. The straight lines indicate the respective fits with the power law with $\tau=2.2$. The values of the Et60S series are shifted by 0.8 and of Et60T by 1.6 along the y-axis for the sake of clarity.

4 CONCLUSIONS

Pure ethanol has different cluster forming properties from the rest of the systems: many smaller sized clusters can be found up to 100 to 370 molecules, depending on the HB condition applied. In this liquid, virtually no percolation occurs. On the other hand, all the studied ethanol-water mixtures have a 3D percolating infinite main cluster, and therefore they form a network. The size of the percolating main cluster is increasing with increasing water concentration, containing 86 to ~100% of the molecules (84 to 99.7% of the ethanol and 94.8 to ~100% of the water molecules). Smaller clusters, <50 molecules, can be found beside the main cluster in these systems; their size and number is decreasing with increasing water concentration. For pure water (almost) all the molecules are in the main

cluster. Ethanol is more prone to be found in smaller binary or pure clusters, or to remain as solitary molecules without hydrogen bonding.

The fractal dimensions of the infinite percolating clusters are increasing from $d_f=2.6$ to 2.9 for the ethanol-water mixtures and $d_f=2.99$ for water, regardless of the choice of the water force field or HB condition: all values are above $d_f=2.53$ predicted by random site percolation theory [25]. This indicates that random site percolation theory can be applied for the description of the percolation behavior of these mixtures, despite the size difference between ethanol and water molecules.

If only the monotype cluster formation is considered (these clusters are mostly part of larger binary clusters), then 3D water percolation is found in the Et20T and Et40T systems, putting the percolation threshold for water in ethanol-water mixtures between 40-60% ethanol content. This is significantly higher than the ethanol content of 10%, suggested before by Sato et al. [5]. There are experimental evidences [1,5,6] that some structural changes occur around ~50% ethanol content, which is in agreement with our findings. Fractal dimensions for the infinite percolating water clusters are between 2.53 and 2.84; these values are above the 3D percolation threshold.

Regarding the choice of the hydrogen bond condition, there are obviously some quantitative differences in terms of the cluster number and size distributions and fractal dimensions, and the exact value of the percolation threshold would be affected, too. However, the statement that 3D percolation exists in these systems in the investigated concentration range is still valid. Therefore qualitatively our findings do not depend on the choice of the applied hydrogen bond condition; it seems to be prudent to use the strictest S150 HB condition, as in this case the connectivities appear to be the most realistic.

Lacunarity analysis [11] and the monotype cluster formation indicate that although microscopic phase separation might occur in these systems, but (as it is well known) macroscopic phase separation is not observable. Although 3D water percolation is present in the ≤ 40 mol % ethanol concentration region, no percolation can be found in pure ethanol and so forth 3D ethanol percolation cannot occur in the mixtures, either. This may explain why ethanol-water mixtures remain miscible over the entire concentration region, as immiscibility seems to occur if both of the components are percolating in 3D separately (cf. Ref. [24]).

ACKNOWLEDGMENTS

This work was supported by the National Research, Development and Innovation Agency (NRDIO; in Hungarian: NKFIH, Hungary), under contract No. SNN 116198.

REFERENCES

-
- ¹ K. Nishikawa, T. Iijima, Small-angle X-ray scattering study of fluctuations in ethanol and water mixtures, J. Phys. Chem. 97 (1993) 10824–10828, <http://dx.doi.org/10.1021/j100143a049>.
- ² N. Nishi, S. Takahashi, M. Matsumoto, A. Tanaka, K. Muraya, T. Takamuku, T. Yamaguchi, Hydrogen bonding cluster formation and hydrophobic solute association in aqueous solution of ethanol, J. Phys. Chem. 99 (1995) 462–468, <http://dx.doi.org/10.1021/j100001a068>.
- ³ G. Onori, Compressibility and structure of aqueous solutions of ethyl alcohol, J. Chem. Phys. 89 (1988) 4325–4332, <http://dx.doi.org/10.1063/1.454816>.

-
- ⁴ M. D'Angelo, G. Onori, A. Santucci, Self-association of monohydric alcohols in water: compressibility and infrared absorption measurements, *J. Chem. Phys.* 100 (1994) 3107–3113, <http://dx.doi.org/10.1063/1.466452>.
- ⁵ T. Sato, A. Chiba, R. Nozaki, Dynamical aspects of mixing schemes in ethanol–water mixtures in terms of the excess partial molar activation free energy, enthalpy and entropy of the dielectric relaxation process, *J. Chem. Phys.* 110 (1999) 2508–2521, <http://dx.doi.org/10.1063/1.477956>.
- ⁶ A. Ben-Naim, Inversion of the Kirkwood–Buff theory of solutions: application to the water–ethanol system, *J. Chem. Phys.* 67 (1977) 4884–4890, <http://dx.doi.org/10.1063/1.434669>.
- ⁷ J. Fidler, P.M. Rodger, Solvation structure around aqueous alcohols, *J. Phys. Chem. B* 103 (1999) 7695–7703, <http://dx.doi.org/10.1021/jp9907903>.
- ⁸ Y. Andoh, K. Yasuoka, Hydrogen-bonded clusters on the vapor/ethanol–aqueous-solution interface, *J. Phys. Chem. B* 110 (2006) 23264–23273, <http://dx.doi.org/10.1021/jp061150k>.
- ⁹ O. Gereben, L. Pusztai, Hydrogen bond connectivities in water–ethanol mixtures: On the influence of the H-bond definition, *J. Mol. Liq.* 220 (2016) 836–841, <http://dx.doi.org/10.1016/j.molliq.2016.05.035>.
- ¹⁰ O. Gereben, Ring structure analysis of ethanol–water mixtures *J. Mol. Liq.* 211 (2015) 812–820, <http://dx.doi.org/10.1016/j.molliq.2015.08.010>.
- ¹¹ O. Gereben, Lacunarity analysis of atomic configurations: Application to ethanol-water mixtures, *Phys. Rev. E* 92 (2015) 033305/1–6, <http://dx.doi.org/10.1103/PhysRevE.92.033305>.

-
- ¹² O. Gereben, L. Pusztai, Investigation of the structure of ethanol–water mixtures by molecular dynamics simulation I: analyses concerning the hydrogen-bonded pairs, J. Phys. Chem. B 119 (2015) 3070–3084, <http://dx.doi.org/10.1021/jp510490y>; O. Gereben, L. Pusztai, Correction to “investigation of the structure of ethanol–water mixtures by molecular dynamics simulation I: analyses concerning the hydrogenbonded pairs”, J. Phys. Chem. B 119 (2015) 4564–4564, <http://dx.doi.org/10.1021/acs.jpcb.5b02167>.
- ¹³ W.L. Jorgensen, D. Maxwell, S. Tirado-Rives, Development and testing of the OPLS all-atom force field on conformational energetics and properties of organic liquids, J. Am. Chem. Soc. 118 (1996) 11225–11236, <http://dx.doi.org/10.1021/ja9621760>.
- ¹⁴ H.J.C. Berendsen, J.R. Grigera, T.P. Straatsma, The Missing Term, The missing term in effective pair potentials, J. Phys. Chem. 91 (1987) 6269–6271, <http://dx.doi.org/10.1021/j100308a038>.
- ¹⁵ J.L.F. Abascal, C. Vega, A general purpose model for the condensed phases of water: TIP4P/2005C, J. Chem. Phys. 123 (2005) 234505/1–12, <http://dx.doi.org/10.1063/1.2121687>.
- ¹⁶ G. Lamoureux, A.D. MacKerell Jr., B. Roux, A simple polarizable model of water based on classical Drude oscillators, J. Chem. Phys. 119 (2003) 5185–5197, <http://dx.doi.org/10.1063/1.1598191>.
- ¹⁷ S.Yu. Noskov, G. Lamoureux, B. Roux, Molecular dynamics study of hydration in ethanol–water mixtures using a polarizable force field, J. Phys. Chem. B 109 (2005) 6705–6713, <http://dx.doi.org/10.1021/jp045438q>.

-
- ¹⁸ B. Chen, J.I. Siepmann, Microscopic Structure and Solvation in Dry and Wet Octanol, J. Phys. Chem. B 110 (2006) 3555, <http://dx.doi.org/10.1021/jp0548164>.
- ¹⁹ A. Vrhovšek, O. Gereben, A. Jamnik, L. Pusztai, Hydrogen bonding and molecular aggregates in liquid methanol, ethanol, and 1-propanol, J. Phys. Chem. B 115 (2011) 13473–13488, <http://dx.doi.org/10.1021/jp206665w>.
- ²⁰ A. Geiger, F.H. Stillinger, A. Rahman, Aspects of the percolation process for hydrogen-bond networks in water, J. Chem. Phys. 70 (1979) 4185–4193, <http://dx.doi.org/10.1063/1.438042>.
- ²¹ H.E. Stanley, J. Teixeira, Interpretation of the unusual behavior of the H₂O and D₂O at low temperatures: tests of a percolation model, J. Chem. Phys. 73 (1980) 3404–3422, <http://dx.doi.org/10.1063/1.440538>.
- ²² A. Geiger, H.E. Stanley, Low-density “patches” in the hydrogen-bond network of liquid water: evidence from molecular-dynamics computer simulations, Phys. Rev. Lett. 49 (1982) 1749–1752, <http://dx.doi.org/10.1103/PhysRevLett.49.1749>.
- ²³ R.L. Blumberg, E. Stanley, Connectivity of hydrogen bonds in liquid water J. Chem. Phys. 80 (1984) 5230–5241, <http://dx.doi.org/10.1063/1.446593>.
- ²⁴ A. Oleinikova, I. Brovchenko, A. Geiger, B. Guillot, Percolation of water in aqueous solution and liquid–liquid immiscibility, J. Chem. Phys. 117 (2002) 3296–3304, <http://dx.doi.org/10.1063/1.1493183>.
- ²⁵ N. Jan, Large lattice random site percolation, Physica A 266 (1999) 72–75, [http://dx.doi.org/10.1016/S0378-4371\(98\)00577-9](http://dx.doi.org/10.1016/S0378-4371(98)00577-9).

²⁶ <http://www.gromacs.org>; D. van der Spoel, E. Lindahl, B. Hess, G. Groenhof, A.E.

Mark, GROMACS: fast, flexible, and free, H.J.C. Berendsen, J. Comput. Chem. 26
(2005) 1701–1718, <http://dx.doi.org/10.1002/jcc.20291>.